Science Translational Medicine
AAAS

stm.sciencemag.org/cgi/content/full/12/539/eaax3799/DC1

Supplementary Materials for

Interleukin 17 and senescent cells regulate the foreign body response to synthetic material implants in mice and humans

Liam Chung, David Maestas Jr, Andriana Lebid, Ashlie Mageau, Gedge D. Rosson, Xinqun Wu, Matthew T. Wolf, Ada Tam, Isabel Vanderzee, Xiaokun Wang, James I. Andorko, Hong Zhang, Radhika Narain, Kaitlyn Sadtler, Hongni Fan, Daniela Čiháková, Claude Jourdan Le Saux, Franck Housseau, Drew M. Pardoll, Jennifer H. Elisseeff*

*Corresponding author. Email: jhe@jhu.edu

Published 15 April 2020, *Sci. Transl. Med.* **12**, eaax3799 (2020)
DOI: 10.1126/scitranslmed.aax3799

The PDF file includes:

Fig. S1. $CD3^+$ T cells are up-regulated in human fibrotic capsule tissue.
Fig. S2. IL17, but not IFNγ or IL4, is expressed in response to implanted synthetic material.
Fig. S3. Expression profile of immune cells surrounding synthetic material implants is proinflammatory.
Fig. S4. Systemic immune homeostasis is influenced by synthetic material implants in mice.
Fig. S5. Type 17 immune response induced by synthetic material is antigen dependent.
Fig. S6. IL17-deficient mice have a reduced fibrotic response to implanted synthetic materials.
Fig. S7. Type 17 immune response regulates the recruitment of myeloid cells.
Fig. S8. IL17 induces development of senescent fibroblasts.
Table S1. List of SYBR Green mouse mRNA primers.
Table S2. List of mouse TaqMan gene expression primers.
Table S3. List of human TaqMan gene expression primers.
Table S4. Antibodies used for flow cytometry (myeloid panel).
Table S5. Antibodies used for flow cytometry (lymphoid panel).

Other Supplementary Material for this manuscript includes the following:

(available at stm.sciencemag.org/cgi/content/full/12/539/eaax3799/DC1)

Data file S1 (Microsoft Excel format). Individual-level data for all figures.

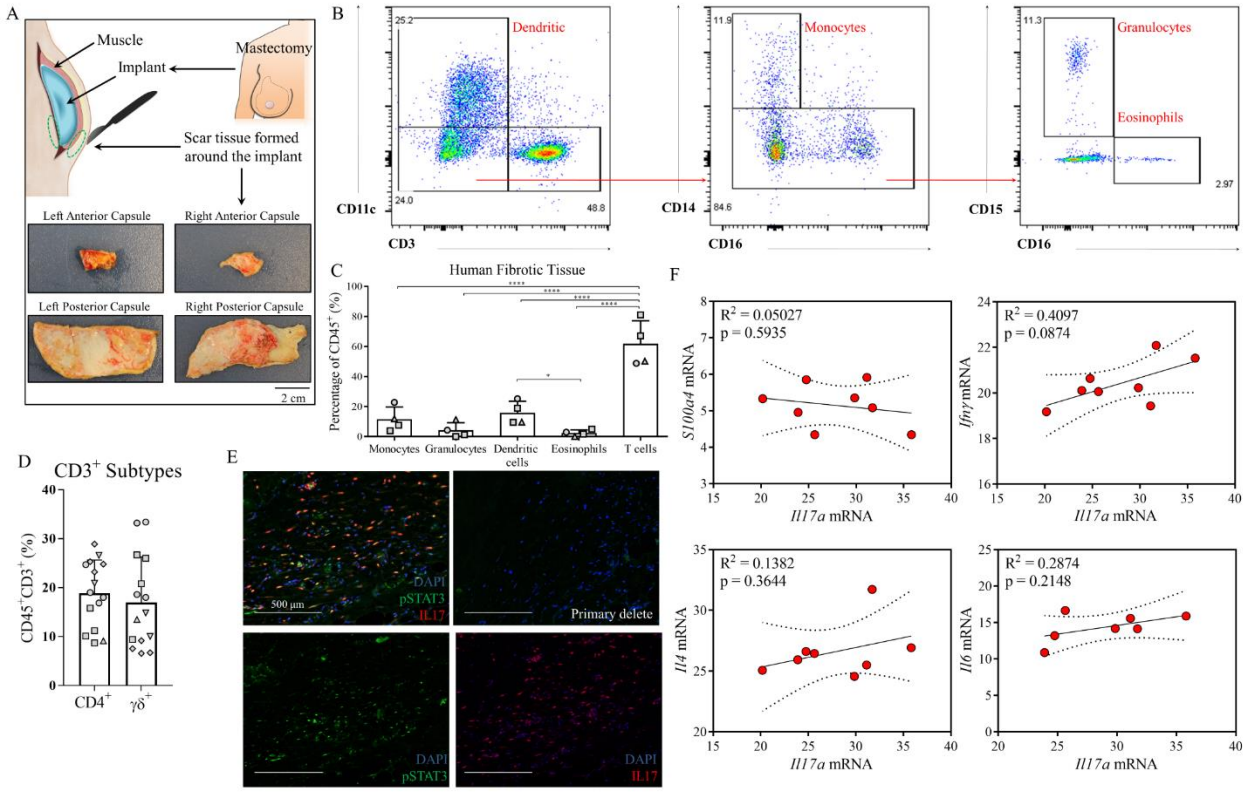

Fig. S1. CD3$^+$ T cells are up-regulated in human fibrotic capsule tissue. (**A**) Illustration of human fibrotic capsule extraction and gross images of the implants. (**B, C**) Representative flow cytometry plot and quantification of myeloid derived cells, including monocytes (CD3$^-$CD11c$^-$ CD14$^+$CD16$^-$), granulocytes (CD3$^-$CD11c$^-$CD14$^+$CD16$^+$CD15$^+$), eosinophils (CD3$^-$CD11c$^-$ CD14$^+$CD16$^+$CD15$^-$), dendritic cells (CD3$^-$CD11c$^+$), and lymphoid derived T cells (CD3$^+$CD11c$^-$). (**D**) Quantification of the percentage of CD4$^+$ T cells and γδ$^+$ T cells in 5 patients. (**E**) Immunofluorescence imaging showing pSTAT3 and IL17 in human fibrous capsule, followed by single staining controls and primary delete. (**F**) Correlation of qRT-PCR gene expression between *Il17a* mRNA and fibrosis-associated genes, including *S100a4*, *Ifnγ*, *Il4*, and *Il6*. Data are mean ± SD, n = 3 (panel C), n = 8 (panel D), n = 5 (panel F). ****P < 0.0001, ***P < 0.001, **P < 0.01, *P < 0.05 by ANOVA for data in panels C, D, or linear regression in panel F.

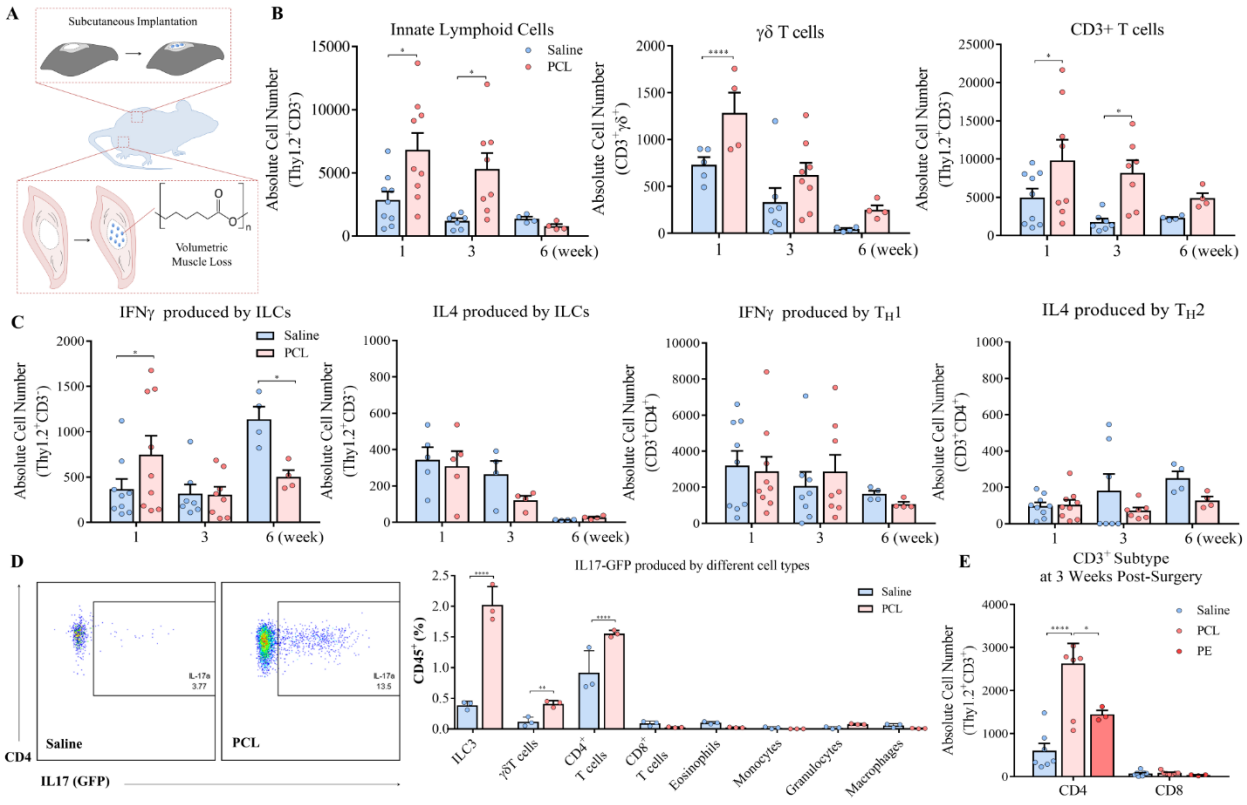

Fig. S2. IL17, but not IFNγ or IL4, is expressed in response to implanted synthetic material. (**A**) Illustration of volumetric muscle loss (VML) and subcutaneous (SQ) implants in the murine model. (**B**) Flow cytometry analysis of the total number of ILCs, $\gamma\delta^+$ T cells, and $CD3^+$ T cells at 1, 3, and 6-weeks post-surgery. (**C**) Kinetics of IFNγ and IL4 expression by ILCs, $\gamma\delta^+$ T cells, and $CD4^+$ T helper cells at various post-injury time points. (**D**) Quantification of IL17A expression across different cell types3-weekspost-surgery in an IL17A-GFP reporter mice. (**E**) Comparison of $CD4^+$ and $CD8^+$ T cells at 3-weeks post-injury with PCL and PE implant. Data are mean ± SD, n = 4-8 (panels B, C), n = 3 (panel D), n = 3-7 (panel E). ****P < 0.0001, ***P < 0.001, **P < 0.01, *P < 0.05 by ANOVA for panel B, C, D, and E.

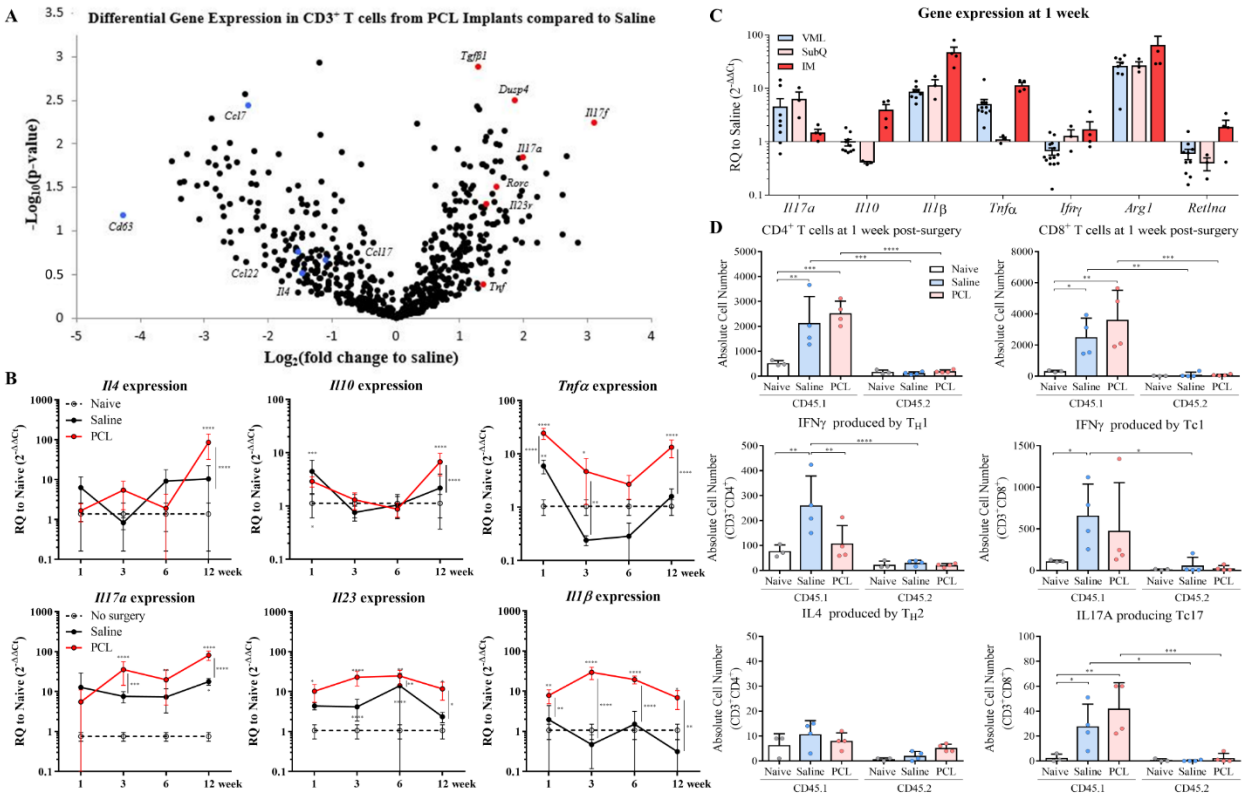

Fig. S3. Expression profile of immune cells surrounding synthetic material implants is proinflammatory. (**A**) $CD3^+$ T cells were sorted for gene expression analysis using the NanoString platform. Volcano plot of genes differentially regulated in PCL-derived T cells compared to saline (no implant) control at day 7 post-surgery. Type 17-associated gene expression differences are highlighted. (**B**) qRT-PCR gene expression normalized to healthy muscle control showing kinetics of *Il4*, *Il10*, *Il17a*, *Il23*, *Tnfα*, and *Il1β* transcripts. (**C**) Gene expression analysis comparing levels of different cytokines between the VML model and subcutaneous (SQ) implant, and intramuscular injection (IM) model at 1-week post-injury. (**D**) Total number of CD4 and CD8 infiltration, T_H1, and T_H2, Tc1, Tc17 from CD45.1 (Wildtype donor) and CD45.2 (OTII-$Rag^{-/-}$ donor) bone marrow chimera mice 1 week after VML. Data are means ± SEM (B), mean ± SD, n = 3-5 (panel B), n = 3-14 (panel C), n = 4 (panel D). ****P < 0.0001, ***P < 0.001, **P < 0.01, *P < 0.05 by ANOVA for panel B, C, and D. Data for Fig. S3A are supplied as a separate Excel file.

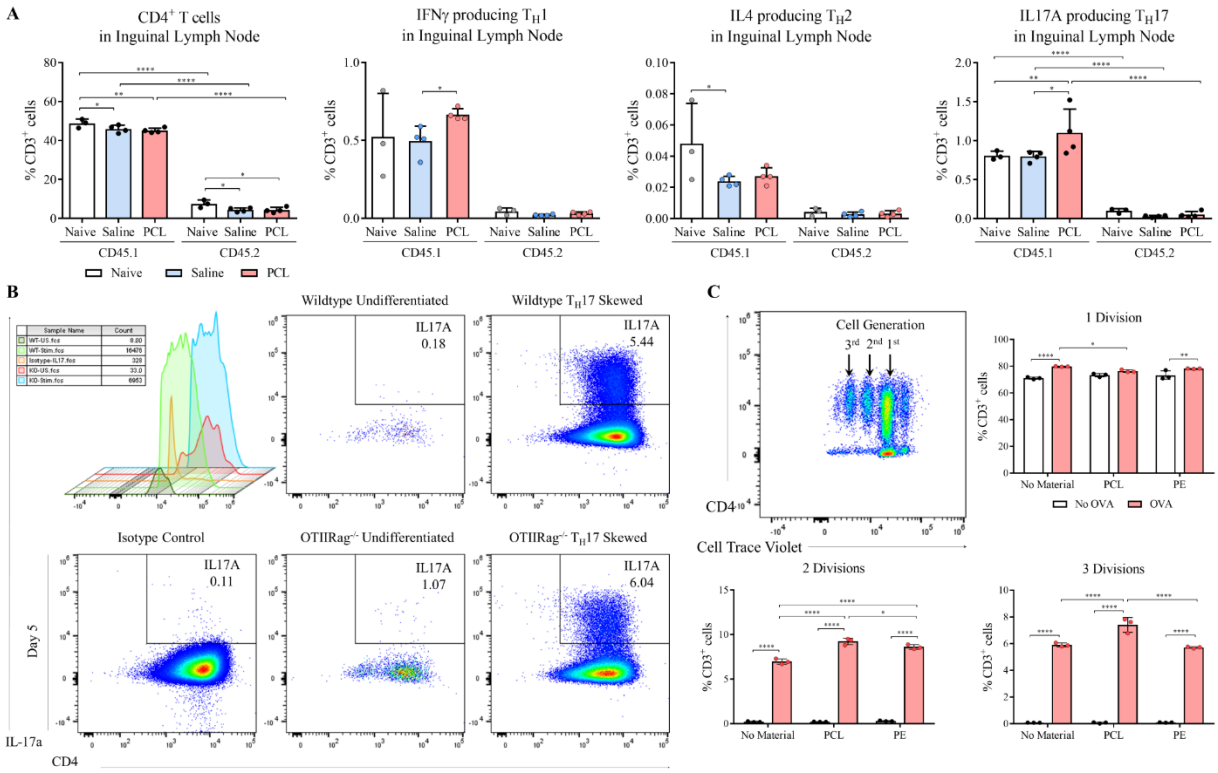

Fig. S4. Systemic immune homeostasis is influenced by synthetic material implants in mice.

(**A**) Total number of immune cells infiltration and T_H17 from CD45.1 (Wildtype donor) and CD45.2 (OTII-Rag$^{-/-}$ donor) bone marrow chimera mice 1 week after VML. Percent of CD4$^+$ T cells, T_H1, T_H2, and T_H17 cells from CD45.1 and CD45.2 in draining lymph nodes were evaluated. (**B**) *Invitro* differentiation of T_H17 cells of OTII-Rag$^{-/-}$ compared to Wildtype naïve CD4$^+$ cells. (**C**) Proliferation assay of T cells co-cultured with splenocytes from OT-II transgenic mice cultured with different materials (PCL or PE) and OVA antigen. Representative plots for proliferation assay were shown. Data are mean ± SD, n = 3-4 (panel A), n = 3 (panel C). ****P < 0.0001, ***P < 0.001, **P < 0.01, *P < 0.05 by ANOVA for panel A, C.

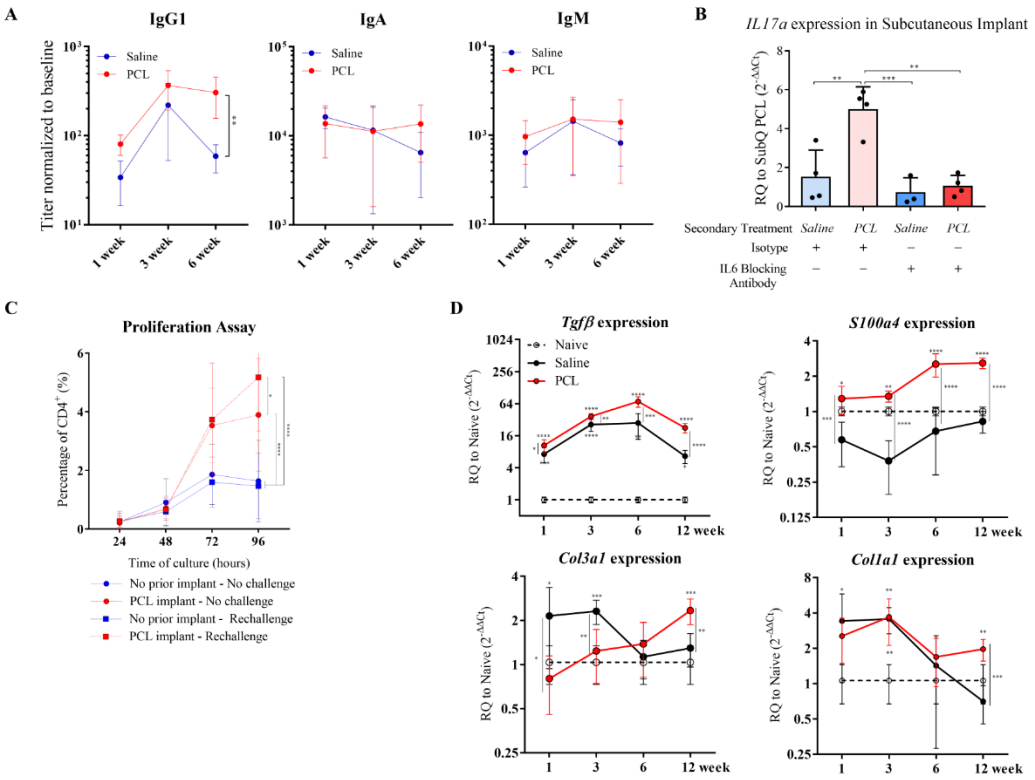

Fig. S5. Type 17 immune response induced by synthetic material is antigen dependent. (**A**) IgG1, IgM, and IgA antibody titers were detected using an enzyme-linked immunosorbent assay (ELISA) system on serum collected 1, 3, and 6-weeks post-surgery and implantation. (**B**) Gene expressions of *Il17a* on SubQ implant in mice previously primed with PCL implant in VML. In addition, neutralizing antibody IL6 (100 μg/mL each mouse per day for 5 consecutive days) or isotype control (rat IgG1) was administered intraperitoneally at 2-weeks post-VML. (**C**) Splenocytes were isolated from mice received initial challenge with PCL implant or saline control. Cells were labeled with CellTrace Violet proliferation dye. In culture, PCL were re-introduced to investigate the memory response. Proliferation were evaluated via flow cytometry at 24, 48, 72, and 96 hours. (**D**) qRT-PCR gene expression normalized to healthy muscle controls showing kinetics of *Tgfβ, S100a4, Col1a1* and *Col3a1* progression in PCL implant mice compared to saline control overtime. Data are mean ± SD, n = 3-5 (panels A, B, D), n = 3-9 (panel C). ****P < 0.0001, ***P < 0.001, **P < 0.01, *P < 0.05 by ANOVA for panel A, B, C, and D.

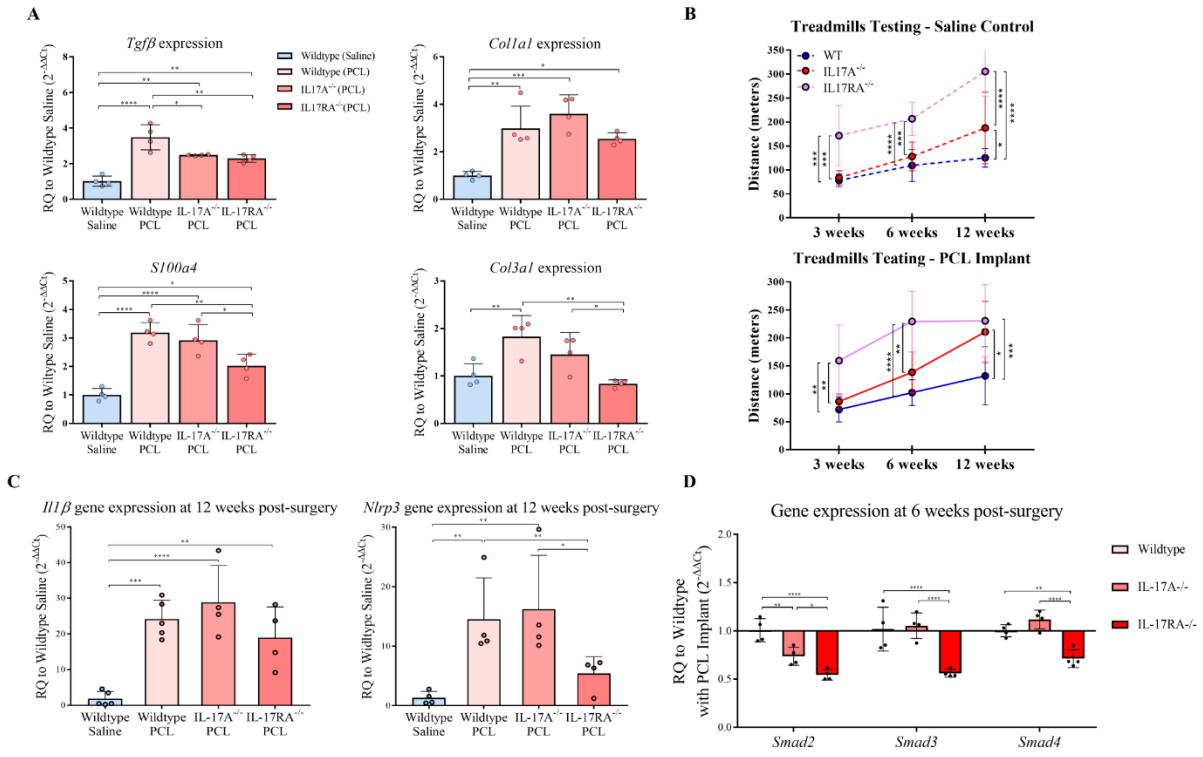

Fig. S6. IL17-deficient mice have a reduced fibrotic response to implanted synthetic materials. (**A**) Gene expression analysis of fibrotic markers in the whole tissue including *Tgfβ*, *S100a4*, and *Col3a1* in Wildtype, IL17A$^{-/-}$, and IL17RA$^{-/-}$ mice at 12-weeks post-surgery. (**B**) Treadmill exhaustion assay 3, 6, and 12-weeks post-implantation of Wildtype, IL17A$^{-/-}$, and IL17RA$^{-/-}$ mice. (**C**) qRT-PCR analysis of inflammasome related genes including Il1β and Nlrp3 was performed in Wildtype, IL17A$^{-/-}$, and IL17RA$^{-/-}$ mice at 12-weeks post-surgery. (**D**) Gene expressions of *Smad2*, *Smad3*, and *Smad4* in Wildtype, IL17A$^{-/-}$, and IL17RA$^{-/-}$ mice at 6-weeks post-surgery were shown. Data are mean ± SD (B), n = 4-5 (panel A, C, D), n = 4-10 (panel B). ****P < 0.0001, ***P < 0.001, **P < 0.01, *P < 0.05 by ANOVA for panel A, B, C, and D.

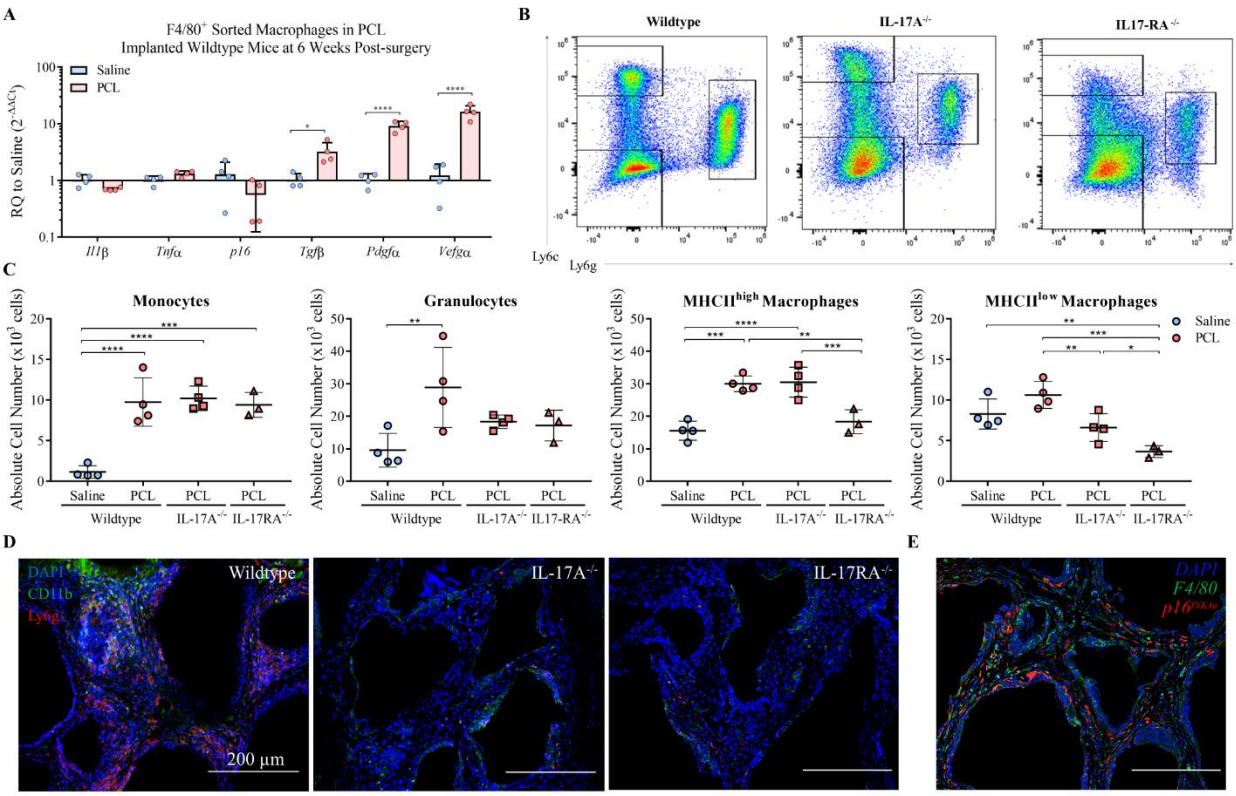

Fig. S7. Type 17 immune response regulates the recruitment of myeloid cells. (**A**) Gene expression analysis of F4/80^{+} cells sorted from PCL implanted Wildtype mice 6-weeks post-surgery. (**B**) Flow cytometry representative plots comparing different populations of myeloid cells in Wildtype, IL17A$^{-/-}$, and IL17RA$^{-/-}$ mice. (**C**) Quantification of granulocytes (CD11b^{+}Ly6intLy6g^{high}), MHCII^{high} macrophages (CD11b^{+}Ly6c^{low}Ly6g^{low}MHCII^{high}F4/80^{+}), MHCII^{low} macrophages (CD11b^{+}Ly6c^{low}Ly6g^{low}MHCII^{low}F4/80^{+}), and monocytes (CD11b^{+}Ly6c^{high}Ly6g^{low}) in Wildtype, IL17A$^{-/-}$, and IL17RA$^{-/-}$ mice after 3 weeks with PCL implants. (**D**) Immunofluorescence imaging of CD11B and LY6G around PCL implants in Wildtype and IL17 signaling deficient mice12-weeks post-surgery.(**E**) Immunofluorescence imaging of F4/80 and p16^{INK4a} in Wildtype mice 12-weeks post-surgery. Data are mean ± SD, n = 4 (panel A), n = 3-4 (panel C). ****P < 0.0001, ***P < 0.001, **P < 0.01, *P < 0.05 by ANOVA for panel A and C.

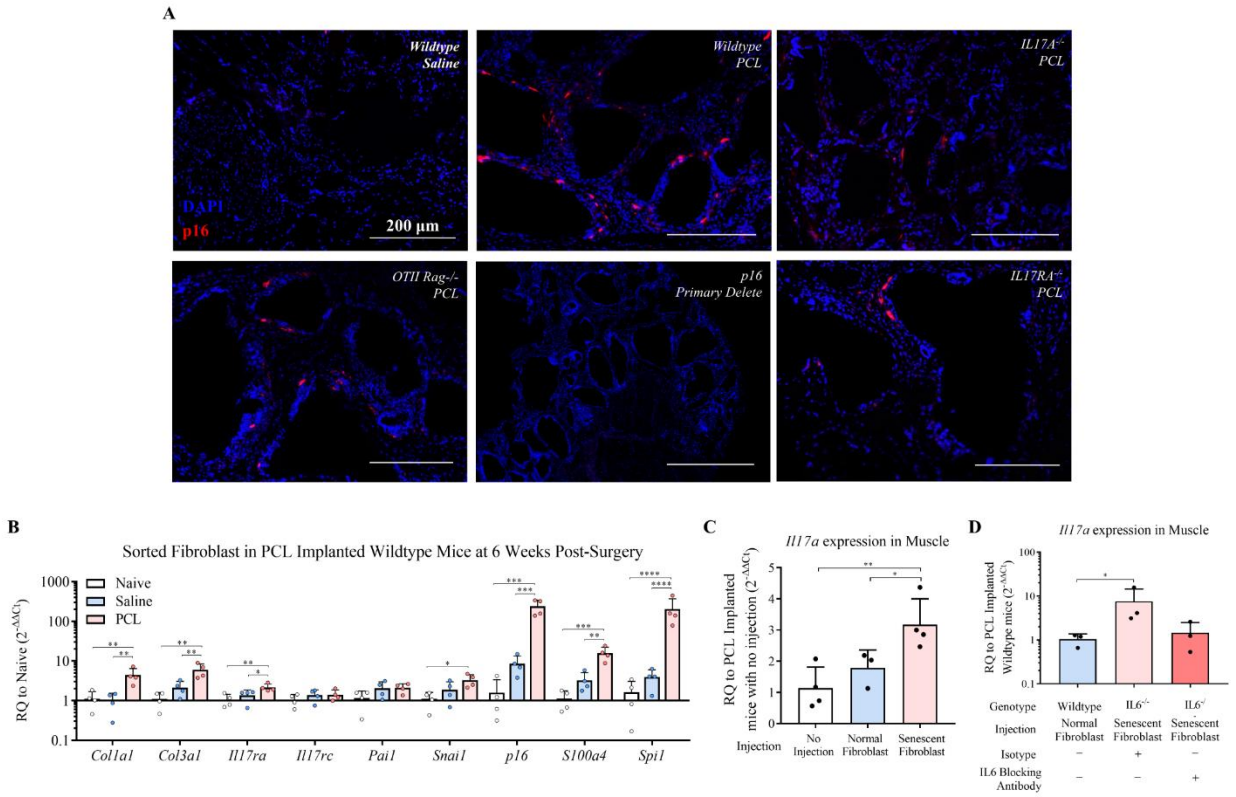

Fig. S8. IL17 induces development of senescent fibroblasts. (**A**) Immunofluorescence staining of $p16^{INK4a}$ (red) in Wildtype, $IL17A^{-/-}$, and $IL17RA^{-/-}$, OTII-$Rag^{-/-}$ mice at 6-weeks post-injury,followed by primary antibody delete control. (**B**) Gene expression analysis of fibroblasts sorted from PCL implanted Wildtype mice 6-weeks post-surgery. (**C**) Gene expressions of *Il17a* in mice that received injection of normal fibroblast or senescent fibroblasts compared to no injection control. (**D**) Gene expressions of Il17a at 1-week post-VML in $IL6^{-/-}$ mice that received injection of senescent fibroblasts compared to normal fibroblasts. Data are mean ± SD, n = 4 (panel B), n = 3-4 (panel C), n = 3 (panel D). ****P < 0.0001, ***P < 0.001, **P < 0.01, *P < 0.05 by ANOVA for panel B, C, and D.

Table S1. List of SYBR Green mouse mRNA primers.

Primer	Forward Sequence	Primer	Reverse Sequence
β2m forward	CTC GGT GAC CCT GGT CTT TC	β2m reverse	GGATTT CAA TGT GAG GCG GG
Tnfα forward	GTC CAT TCC TGA GTT CTG	Tnfα reverse	GAA AGG TCT GAA GGT AGG
Il1β forward	GTA TGG GCT GGA CTG TTT C	Il1β reverse	GCT GTC TGC TCA TTC ACG
Retnla forward	CTT TCC TGA GAT TCT GCC CCA G	Retnla reverse	CAC AAG CAC ACC CAG TAG CA
Ifnγ forward	TCA AGT GGC ATA GAT GTG GAA	Ifnγ reverse	TGA GGT AGA AAG AGA TAA TCT GG
Il4 forward	ACA GGA GAA GGG ACG CCA T	Il4 reverse	ACC TTG GAA GCC CTA CAG A
Il17a forward	TCA GCG TGT CCA AAC ACT GAG	Il17a reverse	CGC CAA GGG AGT TAA AGA CTT
Arginase 1 forward	CAG AAG AAT GGA AGA GTC AG	Arginase 1 reverse	CAG ATA TGC AGG GAG TCA CC
Cdkn2a (p16) forward	AAT CTC CGC GAG GAA AGC	p16 reverse	GTC TGC AGC GGA CTC CAT S
Cdkn2b (p15) forward	AGA TCC CAA CGC CCT GAA C	p15 reverse	CCC ATC ATC ATG ACC TGG ATT
l10 forward	CAG GAC TTT AAG GGT TAC TTG GGT	Il10 reverse	GCC TGG GGC ATC ACT TCT AC

Table S2. List of mouse TaqMan gene expression primers.

Primer	Assay ID:	Primer	Assay ID
β2m	Mm00437762	Il17a	Mm00439618
Col1a1	Mm00801666	Il23a	Mm00518984
Col3a1	Mm00802300	S100a4	Mm00803372
Pai1	Mm00435858	Snai1	Mm00441533
Tgfβ-1	Mm01178820	p16	Mm00494449
Nlrp3	Mm00840904	Smad2	Mm00487530
Smad3	Mm01170760	Smad4	Mm03023996

Table S3. List of human TaqMan gene expression primers.

Primer	Assay ID:	Primer	Assay ID
β2m	Hs00187842	Il17a	Hs00174383
Col1a1	Hs00164004	STAT3	Hs00374280
Col3a1	Hs00943809	S100a4	Hs00243202
p16	Hs00923894	Tgfβ-1	Hs00998133
Cdkn1a (p21)	Hs00355782	Ifnγ	Hs00989291
Il4	Hs00174122	Il6	Hs00174131

Table S4. Antibodies used for flow cytometry (myeloid panel).

Fluorophore	Marker	Manufacturer	Catalogue
Fixable Yellow	Live/Dead	Life Technologies	L34968
AF488	MHC-II	BioLegend	107615
PerCP-Cy5.5	CD11b	BioLegend	101227
APC-Cy7	CD11c	BioLegend	117323
PE-CF594	Siglec F	BDbiosciences	562757
Pacific Blue	Ly6c	BioLegend	128013
AF647	Ly6g	BioLegend	127609
BV510	CD45	BioLegend	103137
PE-Cy7	F4/80	BioLegend	123113

Table S5. Antibodies used for flow cytometry (lymphoid panel).

Fluorophore	Marker	Manufacturer	Catalogue
Fixable eFlour 780	Live/Dead	Life Technologies	65-0865-14
BV786	CD3	BDbiosciences	564010
FITC	CD4	BioLegend	100509
BV711	CD8	BioLegend	100747
PE-CF594	γδ-TCR	BDbioscienes	563532
APC	IFNγ	BioLegend	505809
PE	IL4	BioLegend	504103
AF700	IL17A	BioLegend	506914
BV510	CD45	BioLegend	103137
PE-Cy7	Thy1.2	BioLegend	140309